

---

# Specific Binding of Cancer-derived Exosomes to Synthetic Carbon Beads – Implication for Adjuvant and Neoadjuvant Cancer Treatment

---

Oleta A. Sandiford<sup>1,†</sup>, Sri Harika Pamarthi<sup>1,†</sup>, Marina Gergues<sup>1</sup>, Katherine Redinius<sup>2</sup>, Vanessa Wood Braband<sup>2</sup>, Anish G. Rangdal<sup>1</sup>, Jacob Petersen<sup>3</sup>, Jose Diaz Aunon<sup>2</sup> and Pranela Rameshwar<sup>1,\*</sup>

<sup>1</sup>*Department of Medicine, Rutgers New Jersey Medical School, USA*

<sup>2</sup>*Immutrix Therapeutics, Rapid City, SD, USA*

<sup>3</sup>*South Dakota School of Mines and Technology, Rapid City, SD, USA*

*E-mail: rameshwa@njms.rutgers.edu*

*\*Corresponding Author*

*†These authors contributed equally to this study*

Received 16 April 2025; Accepted 15 May 2025

## Abstract

Extracellular vesicles (exosomes) can mediate intercellular communication. In cancer patients, exosomes are central to intercellular communication between cancer cells and non-malignant cells within the tissue niche, and at distant regions. This type of communication influences the biology of the cancer and treatment response. This study tested the hypothesis that carbon beads, 150–500  $\mu\text{m}$  in size with pore size about 27 nm, can capture exosomes from the plasma of cancer patients, and from a glioblastoma cell line (T98G). The challenge to addressing the hypothesis is the relatively larger size of exosomes, 50–120 nm, to be captured within the carbon pore. This study tested plasma from a patient with ovarian cancer and two breast cancer patients, HER2+ and triple negative for hormone receptor (TNBC),

*International Journal of Translational Science, Vol. 1, 69–90.*

doi: 10.13052/ijts2246-8765.2025.004

© 2025 River Publishers

and released exosomes from T98G cells. This study showed exosomes from ovarian plasma binding to a specific synthetic carbon, C529. Similar binding did not occur with plasma from age-matched healthy controls. GBM exosomes also bound to C529 but the repertoire of carbon was broader. TNBC exosomes showed low affinity for the identified carbon. However, exosomes from HER2+ breast cancer were able to bind to the carbon beads. In total, this study showed binding of exosomes from cancer plasma to C529 carbon. The results of these findings are discussed in the context of potential treatment, and they provide future direction for studies to examine carbon beads as adjuvant or neoadjuvant treatment for cancer.

**Keywords:** Carbon, cancer, stem cell, exosomes, glioblastoma, ovarian cancer.

## Introduction

Exosomes are small extracellular vesicles that are processed in the endosomes of cells. Exosomes are produced by the cells to mediate intercellular communication [1]. The influence of the exosomes on function is due to their molecular cargo. Using breast cancer behavior as an example, exosomes can influence this cancer to adapt dormancy or to reverse dormancy into metastasis [2, 3]. Dormancy can be achieved in the bone marrow when exosomes from cancer cells and bone marrow stromal cells induced changes in both cell sources [2]. Interestingly, in a microenvironment that produce a distinct cue, exosomes are loaded with different cargo and this could lead to reverse dormancy [3].

Exosomes are round and cup shaped vesicles, 50–120 nm in size with proteins, lipids and nucleic acid cargo [4]. Although all cell types can secrete exosomes, the functions of the exosomes depended on the activation cue, source cells, and the ensued intercellular communication. As an example, exosomes released from mesenchymal stem cells (MSCs) will share different cargo relative to the exosomes released after they were primed by the secretome of breast cancer cells [2]. Similarly, exosomes from umbilical cord blood cells change after exposure to secretome from aged hematopoietic cells [5].

Attempts to identify the cellular source of exosomes could be complex. However, there are instances when the exosomes might express molecules of the source cells. It is expected that antigen presenting cells, if activated, could release exosomes with increased expression of the major histocompatibility

complex II [6]. Similarly, exosomes from neural tissues might express tissue specific markers [7]. Exosomes are increased in the circulation of cancer patients and this might be attributed to their release from both the cancer cells and the affected tissue [8]. The presence of exosomes in cancer is critical to the progression of the tumor [9]. Due to the heterogeneity of tumor cells, it would be a challenge to eliminate cancer-derived exosomes for therapy and research. We propose that cancer exosomes could be removed from the circulation of patients by an extracorporeal method that can capture specific exosomes. This could be done by synthetic porous carbon beads. This was tested using different carbon beads with the goal of identifying carbon that could efficiently remove cancer exosomes. This approach would be highly significant since it could be used as neoadjuvant treatment for a better outcome for subsequent standard of care. In addition, the filtering system could be also used as an adjuvant treatment for cancer.

This study showed binding of exosomes to a specific synthetic carbon. Interestingly, the carbon seemed to be mostly specific to the cancer cells with limited binding to healthy exosomes. The studies identified specific carbon that showed high efficiency with respect to binding cancer-derived exosomes. We report on studies that compared exosomes from a glioblastoma (GBM) cell line with plasma from an ovarian cancer patient. The data indicated that GBM exosomes could bind to a wider range of carbon whereas exosomes from ovarian cancer was limited to a selected few carbon beads. Triple negative breast cancer (TNBC) exosomes showed low efficiency for the identified carbon. However, exosomes from HER2+ breast cancer were able to bind to the carbon beads. The results of these findings are discussed in the context of potential treatment.

## **Materials and Methods**

### **Reagents**

Fetal bovine serum (FBS), tissue culture grade PBS (pH 7.4), Dulbecco Modified Eagle Medium (DMEM), RPMI 1640, L-glutamine (2 mM), penicillin–streptomycin (2 mM), bovine serum albumin (BSA) and phosphatase inhibitor cocktail 2 were purchased from Millipore Sigma (St. Louis, MO), FBS Premium Select from Atlanta Biologicals (Lawrenceville, GA), exosome-depleted FBS from System Biosciences (Palo Alto, CA), and FM 1-43 from Invitrogen (Carlsbad, CA). Dextran-coated carbon beads were provided by Intrinsic (Rapid City, SD).

### Cell Lines

T98G cells were obtained from American Type Culture Collection (ATCC) and cultured as per their instructions. All cell lines were authenticated with ATCC STR database ([www.atcc.org/STR\\_database.aspx](http://www.atcc.org/STR_database.aspx)), in addition to weekly assessment for mycoplasma.

### Human Subjects

Rutgers Institutional Review Board (IRB) approved the use of bone marrow aspirates from healthy donors (18–35 yrs), and blood from ovarian and breast cancer patients (Table 1). All subjects signed the informed consent form.

**Table 1** Ovarian and breast cancer patients

Patient	Age (yrs)	Ethnicity	Diagnosis	Treatment
1	60	Caucasian	Ovarian	Doxorubicin, carboplatin
2	36	Caucasian	Relapse Her2+	
3	Not provided	Caucasian	Triple negative	Adriamycin

### Culture of Human Mesenchymal Stem Cells (MSCs)

MSCs were expanded from bone marrow aspirates, as described in [4]. Briefly, the unfractionated aspirates were diluted in DMEM with 10% FCS and then added to vacuum gas plasma-treated plates (BD Falcon; Franklin Lakes, NJ). After 3 days, red blood cells and granulocytes were removed by Ficoll-Hypaque density gradient centrifugation. The mononuclear fraction was replaced in the plates in media with 50% of the culture media and 50% freshly prepared culture media. At weekly intervals, fresh media replaced 50% of the culture media. The adherent cells were serially passaged at 80% confluence. At passage 4, the cells were negative for CD34, CD45 and CD14; positive for CD29, CD73, CD90, CD105 and CD44, and differentiated into adipogenic and osteogenic cells [10].

### Exosome Isolation

The method to isolate exosomes has been previously described [3, 4, 11]. Exosomes were isolated from the media of MSCs or T98G GBM cells as follows:

### Cell culture media

MSCs and T98G cells, at 90% confluence, were incubated with DMEM containing 2% exosome-free FCS. After 48 h, the media were collected

and then used to isolate exosomes by differential centrifugation as described in [2].

#### **Differential centrifugation**

Cells were cleared from the culture media by centrifuging at 2000 *g* for 20 min. The cell-free supernatants were transferred to sterile 1.5 ml tubes to clear any remaining cell debris and large vesicles by centrifuging at 10,000 *g* for 30 mins. The resulting supernatants were transferred to 5- or 30-ml ultracentrifuge tubes (Thermo Fisher). The supernatants were centrifuged at 100,000 *g* for 80 mins. The supernatants were aspirated and the pellets, which contained the exosomes, were washed with PBS. After this, the exosomes were further centrifuged at 130,000 *g* for 80 min. The pellets were resuspended in 200  $\mu$ l of sterile PBS.

#### **Exosome Quantitation**

The size and number of exosomes were determined using nanoparticle tracking analysis (NTA) (Nanosight, Malvern). The NTA uses light scattering and Brownian motion, a syringe pump, and a script control system. The NanoSight LM10 system, which is equipped with a 405-nm laser, recorded videos. The NTA software (NanoSight version 2.3) analyzed the data.

#### **Flow Cytometry**

Purified exosomes were analyzed for markers by incubating with anti-CD63 Dynabead (Invitrogen,) according to manufacturer's protocol. Briefly, we incubated the purified exosomes with anti-CD63-PE Dynabeads overnight at 4 °C. After this, we selected the beads with a magnetic separator and then labelled them with anti-CD90-APC, -CD63-PE and -CD9-PerCP Cy5.5 at 1/100 final dilution, 30 mins at room temperature. After one wash with PBS, we analyzed the labeled beads on the FACS Calibur. We incubated anti-CD63 to validate the specificity of the beads. After binding, there were additional CD63 sites on the exosomes, as suggested by the manufacturer of the beads.

#### **Washing of Carbon Beads**

Prior to binding with exosomes, the carbon beads were washed with 1× PBS (pH 7.4). The carbon was mixed about 5–10 times by inverting the tubes. After this, the beads were pelleted by centrifugation for 5 mins. The washing was repeated twice.

### **Isolation of Plasma Exosome**

Exosomes from human plasma were isolated with the Total Exosome Isolation Kit (Thermo Fisher). The procedure followed the manufacturer's instruction.

### **Exosome–Carbon Bead Coupling**

#### **Plasma**

Plasma from patients (Table 1) and the age-matched healthy control were diluted at 1/10 in 1× PBS. The diluent (2.5 mL) was added to 100 mg of washed carbon followed by incubation at room temperature for 24 h. During the incubation period, the mixture was subjected to continuous mixing on a rotator. After incubation, the sample was centrifuged at 500 *g* for 5 mins at room temperature. The supernatant, which contained the unbound exosomes, was transferred to a fresh tube. The pellet was resuspended in 200  $\mu$ L of 1× PBS and the mixture boiled for 10 min at 95 °C to detach the bound exosomes. The sample was centrifuged for 5 mins at 500 *g* and the supernatant contained the bound exosomes. The unbound and bound exosomes were quantitated by NTA (see above).

#### **Isolated exosomes**

Washed carbon was incubated with different amounts of exosomes for 1 or 24 h. In the case of GBM exosomes ( $10^{10}$ ), the particles were incubated with 50 mg of carbon for 24 h.

### **Priming of Carbon Beads**

The carbon was washed as described above. During incubation with exosomes, the solution was PBS, DMEM, DMEM with 2% FCS or 4% BSA.

### **DNA Extraction**

DNA was extracted from unbound fraction and bound exosomes with a DNA extraction and purification kit (Qiagen, Germantown, MD).

### **Protein Array**

The exosomes were characterized using a protein array with known markers of exosomes. The arrays were purchased from System Biosciences (Palo Alto, CA). The membranes were analyzed with samples that were sonicated

and samples that were not sonicated. Both samples were heated at 95 °C for 30 mins. One sample was sonicated for 1 h. Both samples were analyzed using manufacturer's recommendations.

### **Transmission Electron Microscopy (TEM)**

The Core Imaging Lab of Robert Wood Johnson Medical School, Rutgers University (Piscataway, NJ) performed the TEM analyses with the provided exosomes. The method was performed at the Core Imaging Lab of Robert Wood Johnson Medical School, Rutgers University (Piscataway, NJ), as described in (2, 4). Briefly, exosomes were added to formavar carbon coated grids and then stained with PTA (phosphotungstic acid). The grid was scoped on a JEOL 1200EX electron microscope and digital images were obtained using advanced microscopy techniques (AMT camera) (Woburn, MA).

### **Scanning Electron Microscopy (SEM)**

SEM analysis was conducted using a Zeiss Supra 40 VP field emission gun system, located at the South Dakota School of Mines and Technology (Rapid City, SD). Carbon beads were mounted directly to adhesive carbon tape, and separately, beads were also fractured and mounted to observe internal porosity. All images were collected using secondary electrons with an accelerating voltage of 8 keV.

### **Statistical Analysis**

Statistical analysis applied ANOVA and the Tukey–Kramer multiple comparisons test.  $P < 0.05$  was considered significant.

## **Results**

### **Exosome Characterization**

We characterized exosomes using several methods. NTA analyses indicated that the exosomes were less than 120 nm (Figure 1A). Electron microscopy validated the report of round and cup shaped particles for exosomes (Figure 1B) [2, 4]. We assessed the exosomes for known proteins with an array. Since proteins can be on the surface and internal, we assessed sonicated and whole (not sonicated) exosomes. Both analyses identified an increase

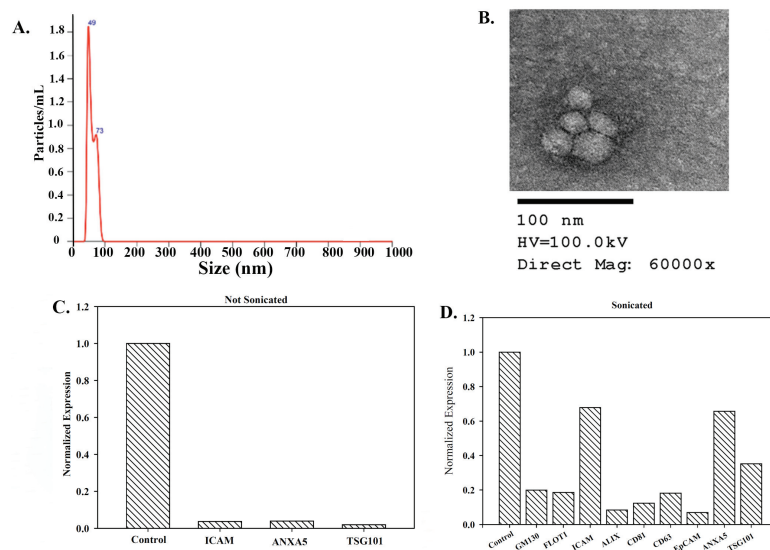


**Figure 1** Characterization of exosomes. (A) Representative histogram of exosomes using the Nanosight. (B) SEM of isolated exosomes. (C) and (D) Protein array analyses of exosomes that were not subjected to sonication (C) and sonicated exosomes (D).

in ICAM (Figure 2C). Since the array was performed with exosomes from MSCs, we were not surprised that ANXA5 was increased. ANXA5 has been reported to be increased in MSCs from bone marrow and umbilical cord [12].

### Binding of MSC-derived Exosomes to Synthetic Carbon Particles

In this section, we ask if carbon particles could bind to exosomes. The first set studies used MSC-released exosomes since this source of exosomes is well-studied [2, 3]. We used MSCs from healthy human bone marrow aspirates. Eight different carbon beads were incubated with  $10^8$  exosomes for 1 h at room temperature. The recovered particles from the carbon (bound) were assessed by NTA. The results indicated efficient binding by C529 (Figure 2A).

### Recapitulating an in vivo Condition with C529

We repeated the studies to recapitulate a scenario in which the carbon particles could be used to absorb exosomes in human circulation. The information was extrapolated from the clinical data shared by Immutrix for dogs. Considering that humans have approximately 5 L (5000 mL) of blood and estimating

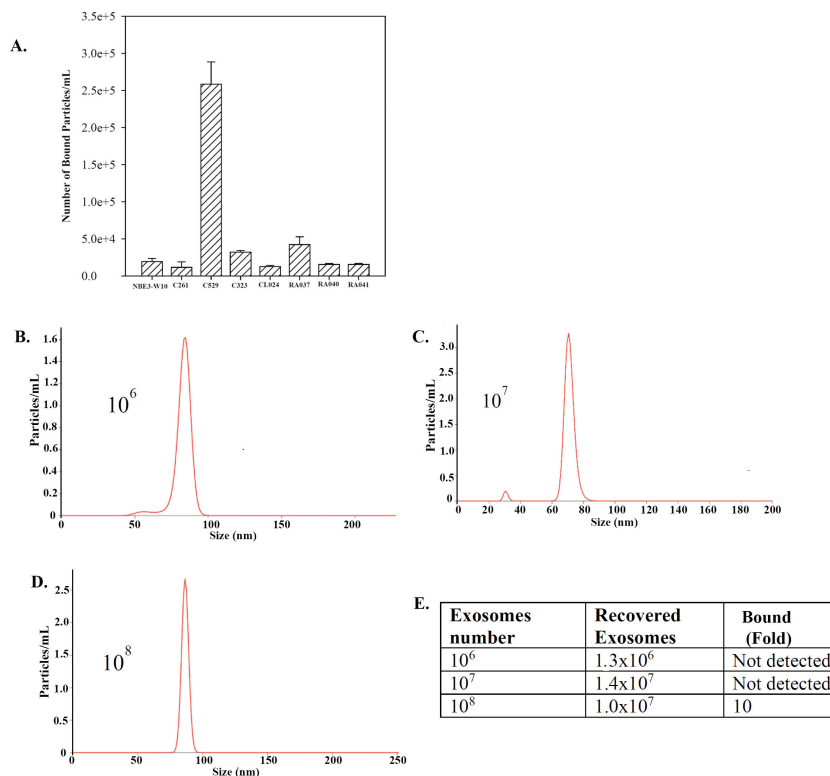


**Figure 2** Bound MSC-derived exosomes to different synthetic carbon particles. (A) Shown are the mean  $\pm$  SD ( $n = 3$ ) number of bound exosomes (particles)/mL for various carbon sources. (B)–(D) Histograms of bound exosomes/particles following incubation of carbon 529 (C-529). The number of added exosomes are shown within the graphs.

100 g beads for 5000 mL of blood, we deduced that 0.02 g beads will be able to capture exosomes from 1 mL blood. We therefore proceeded with 0.02 g beads in 1 mL volume with different  $\log_{10}$  fold exosome particles.

Washed C529 beads (0.02 g) were resuspended with  $10^6$ ,  $10^7$  or  $10^8$  exosome particles in 1 ml of PBS, as described in the materials and methods section. The exosomes were incubated with carbon beads for 1 h. After this, we quantified the bound carbon by NTA. The recovered exosomes are shown in the histograms in Figures 2B and 2D. The inset within each graph identifies the number of added exosomes. The percentage of bound exosomes to C529 was proportional to the total number of input exosomes (Figure 2E).

These findings indicated that a longer incubation period was needed; hence subsequent studies used 24 h incubation.

### **Exosome–Carbon Particle Interaction**

SEM showed a seeming smooth surface of the carbon beads (Figure 3A). Imaging of a single carbon bead indicated pore area with rough surface (Figure 3B, left image). Shown is a focused image of the rough area on the carbon (Figure 3B, right image). The structure of the intact carbon was shown by a distinct SEM image of carbon dust (Figure 3C).

We further examined the interaction between the carbon beads and interaction with exosomes. We labeled the exosomes with the fluorescence dye, FM 1-43, prior to incubation with C621 carbon. SEM imaging of a single carbon indicated binding between the carbon and the labeled exosomes (Figure 3D). In summary, this section showed evidence of binding between exosomes and carbon beads.

### **Interaction of GBM Exosomes with Carbon**

Thus far, the data showed binding between MSC-derived exosomes and carbon particles (Figures 2 and 3D). We asked if exosomes from other cellular sources could also bind to carbon beads. We tested exosomes from T98G/GBM cells and different carbon beads. Unlike MSC exosomes that showed efficient binding to C529, GBM exosomes bound to five carbon materials, including C529 (Figure 3E). Figure 3F showed the size of C529 and the pore size. A pore size of 27 nm on the carbon surface of 250–500  $\mu\text{m}$  indicated that the exosomes could have several pores where they could be captured.

We repeated the studies with 10-fold more exosomes and compared C529 with another carbon, RA003 ( $10^{10}$ ). RA003 showed 1.3-fold more binding to GBM exosomes, as compared to C529 (Figure 4B). Since C529 showed efficient binding to exosomes from GBM and MSCs, we proceeded with C529 carbon.

### **Binding of Exosomes from Ovarian Cancer Plasma to C529**

The MSCs were healthy cells and T98G was a cell line. We therefore asked if C529 can capture exosomes from the plasma of cancer patients. This question was based on the ability of exosomes to mediate communication among cells to benefit the cancer cells [13]. We studied plasma from an ovarian cancer

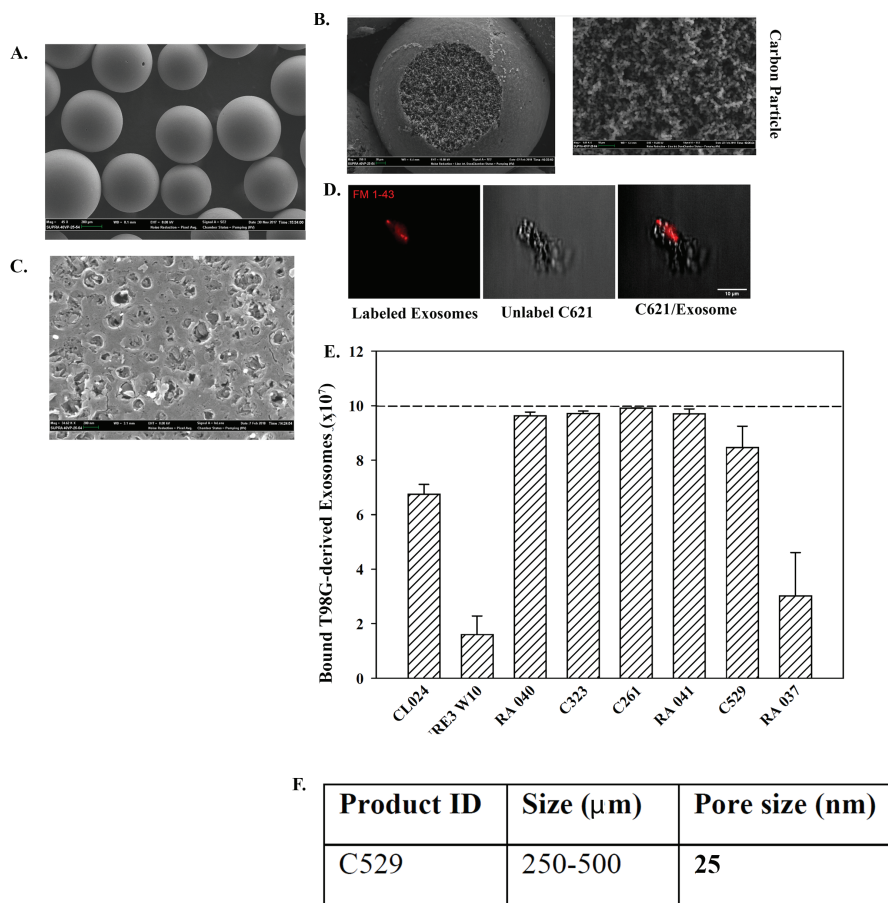


**Figure 3** Bound GBM released exosomes to different carbon particles. (A) SEM of carbon beads. (B) Higher magnification of a carbon bead (left) and an expanded region of the rough region of the bead. (C) SEM of the carbon dust. (D) SEM of carbon bound to fluorescein labeled exosomes. (E) Binding of  $10^7$  exosomes from T98G to different carbon beads. The data are presented as the mean  $\pm$  SD of three independent studies.

patient prior to surgery (pre-surgery). We incubated the plasma with C529 for 16 h. Quantitation of the bound exosomes indicated significant ( $p < 0.05$ ) binding of plasma exosomes to C529, relative to age-matched healthy control (Figure 4C).

DNA is expected in the blood of cancer patients [14]. We therefore asked if C529 could also interact with circulating DNA. To address this

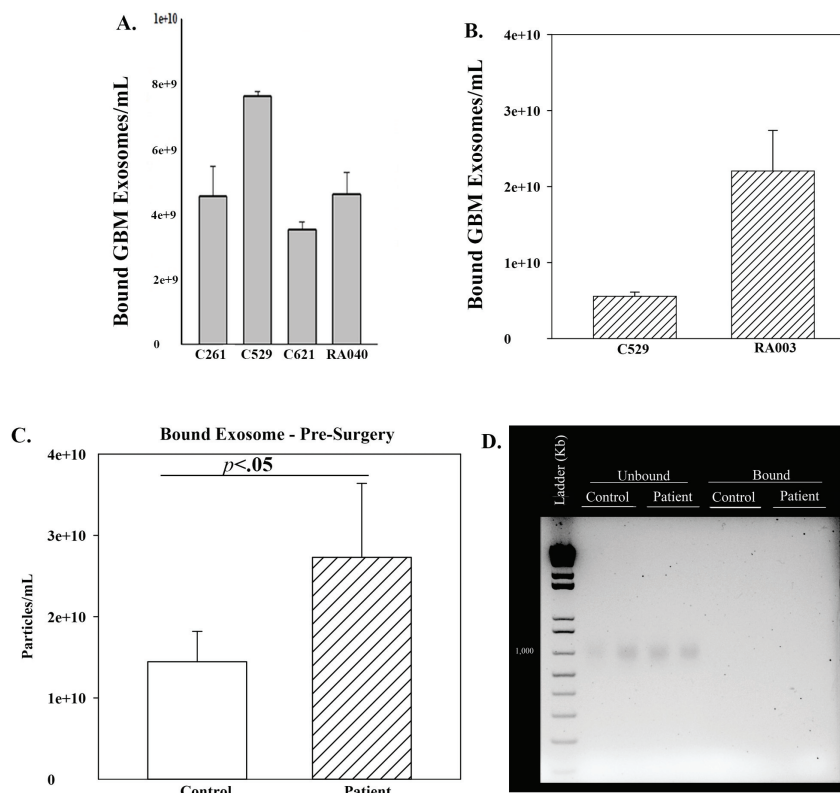


**Figure 4** GBM exosome binding to different carbon beads and binding of exosomes from a patient with ovarian cancer. (A) Exosomes ( $10^9$ ) from T98G cells binding to different carbon beads. The results are presented as the mean  $\pm$  SD of three independent studies. (B) The studies in (A) were repeated with 10-fold more exosomes and the results similarly presented. (C) C529 was incubated with plasma from a patient with ovarian cancer prior to surgery (pre-surgery). Parallel studies used plasma from an age-matched healthy control. The studies were repeated three times and the data presented as the mean  $\pm$  SD. (D) Representative agarose gel with bound exosomes and unbound fraction.

question, we determined whether the carbon could also bind DNA. Exosomes can have DNA cargo and, in the case of cancer patients, it is possible that DNA could be coupled to exosomes [15]. We extracted DNA from bound plasma exosomes (sonicated or not sonicated). Parallel DNA extraction was performed with the unbound fraction. The samples were electrophoresed on 2% agarose gel containing ethidium bromide. We compared the patient plasma with plasma from an age-matched healthy donor. We observed single

supercoiled bands in the unbound fraction but not for the bound exosomes (Figure 4D). These findings suggested specificity of C529 for exosomes.

### **Timeline Binding of Exosomes and C529 in the Plasma of an Ovarian Cancer Patient**

We tested the plasma of the ovarian cancer patient at various times before surgery, post-surgery prior to chemotherapy, and during chemotherapy (Table 1). Plasma exosomes at pre-surgery and during the early period of post-surgery showed strong binding to C529 (Figure 5A). There was a timeline decrease in bound exosomes post-surgery without treatment, consistent with reduced tumor burden (Figure 5A). At the time when the patient was given chemotherapy the number of bound exosomes were reduced to levels similar to age-matched healthy control (Figure 5A).

### **Reduced Binding of Healthy Exosomes to C529 Carbon Beads**

It was important to determine if C529 carbon beads were specific to exosomes from cancer plasma. To address this, we repeated the binding studies with healthy plasma or PBS using C529 and RA003 carbon beads. PBS resulted in undetectable exosomes for both studies (Figure 5B). However, significantly ( $p < 0.05$ ) more healthy exosomes bound to RA003 as compared to C529. Based on these findings, we deduced preferential binding of cancer exosomes to C529.

### **Characterization of Bound Exosomes**

We tested the ovarian exosomes that were retrieved from C529 for CD63, which is a known marker of exosomes. We analyzed the exosomes by flow cytometry with CD63-linked Dynabeads. The plasma exosomes were identified with FITC labeled anti-CD63. The results validated the bound particle as CD63+ (Figure 5C).

### **Influence of Bound Exosomes on Primed Carbon**

C529 and C621 were developed with the same formulation and were expected to be functionally similar. However, these two carbon beads differed with respect to binding GBM exosomes (Figure 4A). Since the binding studies washed the carbon beads with PBS, followed by air drying, we asked if this could account for the varied function/binding. Intrinsic subjected their

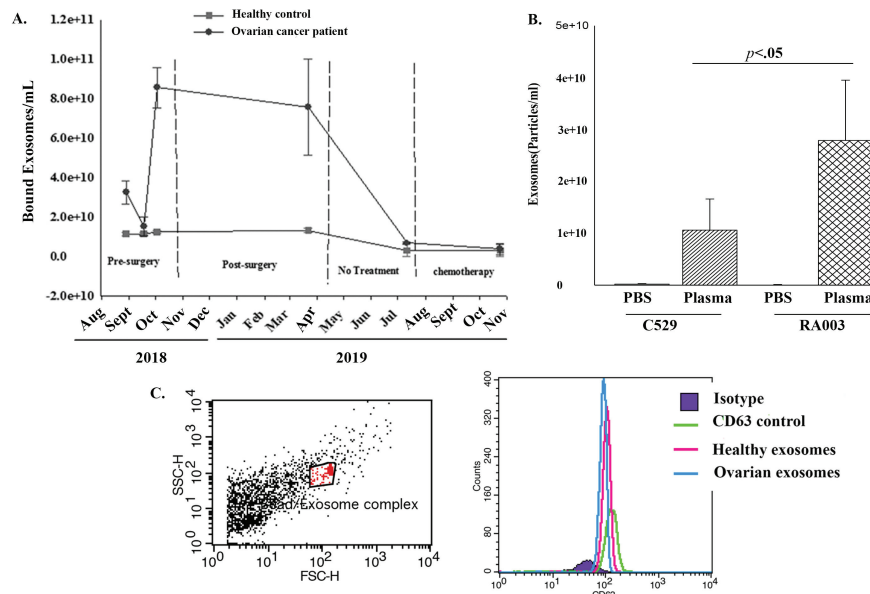


**Figure 5** Timeline changes in bound exosomes from plasma of ovarian cancer patient. (A) Shown are the timeline exosome particles pre- and post-surgery. The latter included the period before and after treatment. Also shown is the timeline study of plasma from age-matched healthy control. Each experimental point was repeated three times. The data represent the mean  $\pm$  SD. (B) Binding of exosomes to healthy plasma and PBS to two different carbon beads. The results are presented as the mean  $\pm$  SD of three experimental repeats. (C) Representative flow cytometry with exosomes isolated from the plasma of a patient with ovarian cancer and age-matched healthy control.

carbon to extensive drying using their protocol. We tested C529 and C621 that were subjected to different washing conditions (Table 2). Comparative results indicated comparable values for N2, bulk density, and PZC (Table 2). Since carbon beads can eliminate B-12, we applied this system to determine relative performance of the three experimental carbon (Table 2). The results showed similar levels of B-12 absorbance (Figure 6A). We therefore deduced that the priming of carbon beads could control capturing of exosomes.

### Binding of Exosomes from Breast Cancer Plasma to C529 Carbon Beads

C529 carbon bound to exosomes from two different solid tumors, T98G GBM cells and ovarian cancer. We asked if C529 could bind exosomes from breast

**Table 2** Nitrogen report of C529 and C621

C529 Archived Data	C529 Stored in PBS; Not Washed	C529 Washed in PBS; Air Dried	C621 Washed and Dried at Intrinsic
Surface area: 565 m <sup>2</sup> /g	Surface area: 569 m <sup>2</sup> /g	Surface area: 575 m <sup>2</sup> /g	Surface area: 573 m <sup>2</sup> /g
Pore size: 26 nm	Pore size: 27 nm	Pore size: 28 nm	Pore size: 28 nm
Bulk density: 0.47 g/mL	Bulk density: 0.53 g/mL	Bulk density: 0.562 g/mL	Bulk density: 0.562 g/mL
PZC: not available	PZC: 7.05	PZC: 6.96	PZC: 7.06

PZC: Point of zero charge

The dried intrinsic carbon was washed and dried overnight at 150°C.

cancer plasma. We studied plasma from HER2+ and TNBC patients. Purified exosomes indicated C529 binding to exosomes from HER2+ breast cancer but not from TNBC (Figures 6C and 6D).

### **Relative Protein Levels from Bound and Unbound Exosomes from Patient Plasma**

We surmised that exosomes could be attached to the surface of carbon beads by increased protein on the exosomes. We quantitated total proteins on bound and unbound exosomes from the plasma of the ovarian cancer patient. Control studies used plasma from age-matched healthy control. The results were normalized to 10<sup>8</sup> exosomes. The data indicated higher levels of protein on bound exosomes, relative to unbound exosomes (Figure 6E).

### **Discussion**

We reported on preferential binding between exosomes from the plasma of ovarian cancer patients and C529 carbon beads (Figures 5 and 6). Similar studies with exosomes from age-matched healthy control did not show significant binding with C529 carbon. Together, the findings strongly suggest that C529 carbon beads were specific for ovarian cancer exosomes. Similar binding studies with exosomes from the culture media of T98G GBM cells indicated that exosomes from GBM have a broader affinity of multiple carbon beads, including C529 (Figure 3E). Further studies with plasma from two breast cancer patients indicated that exosome binding depended on the hormone status of the cancer. Exosomes from the plasma of HER2+ breast cancer

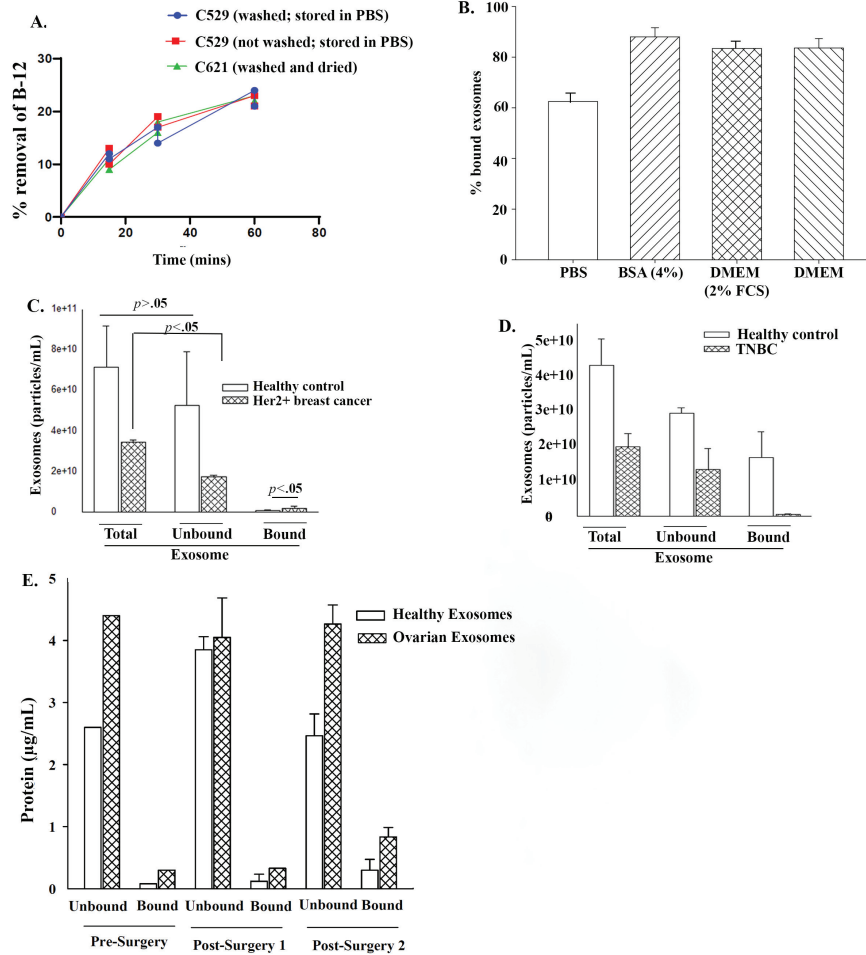


**Figure 6** Priming of C529 for optimized exosome binding and binding with exosomes from breast cancer plasma. (A) Shows the performance test of different washing conditions (Table 2) in assay to assess known binding molecule, B-12. (B) C519 was washed and then air dried. The carbon beads were incubated with  $7 \times 10^{11}$  exosomes from MSCs in solutions shown on the Y-axis. The results are the mean  $\pm$  SD of three independent studies. (C) and (D) The binding studies were performed with exosomes from plasma from a HER2+ breast cancer patient (C) or from a patient with triple negative breast cancer (TNBC). The results showed the total number of exosomes added to the culture and the recovered (unbound) and bound carbon The studies were repeated three times in independent experiments. (E) Total protein levels in bound and unbound exosomes at pre- and post-surgery.

interacted with C529 (Figure 6C). In contrast, there was no difference in the binding between exosomes from TNBC plasma and age-matched healthy control (Figure 6D).

The binding studies indicated that the preparation of the carbon might dictate the binding (Table 2). Such preparation was specific for exosome binding since there was no difference when the varied washes were used to test binding of an established molecule, B12 (Figure 6A). After washing the carbon beads with air drying, we failed to determine if there was weight change, and to determine if the possibility of weight change influenced the results. Nonetheless, this set of studies was insightful since the data suggested that the type of wash followed by air dry might affect how the carbon pore accommodates the exosomes. The exosomes were significantly larger than the pore size (Figure 2E). We surmised methods by which the exosomes might bind to the smaller pore size based on other studies. The main question is, how are exosomes that are about 100 nm able to fit into the 27 nm pore size of the carbon?

The pore size of the carbon is proportional to the size of the beads (Table 3). However, the binding of exosomes seem to be independent of the pore size since the carbon with relatively smaller surface area and pore size (C529) showed preferential binding. It appears that the carbon meso and macro pore size may have an impact, but the data is not linear. This study has limited data to conclude a correlation between pore size and exosome binding. One significant report showed connexin 43 within exosomes [16, 17]. Since connexins are junction proteins, it is possible that this junction function could be part of the increased proteins noted in the bound exosomes (Figure 6E). Electron microscopic images of the exosomes indicated that the vesicles could be cup shaped. This indicated that exosomes could collapse

**Table 3** List of carbon particles

NBE3-W10		RA037
C261		RA040
C529		RA041
C232		RC 069(C621)
CL024		
RA003		
Carbon	Pore Size (nm)	Specific Surface Area (BET, m <sup>2</sup> /g)
C529	25	565
RA040	50	1615
RA041	105	1726

with the appropriate size to fit into the pores (Figure 1). In other models, 3  $\mu\text{M}$  mitochondria can pass through the gap junction with  $\sim 900$  Dalton pore size [18]. Exosomes can form cup shaped structures to fit within the pores.

Exosomes can be released from cancer cells and other tissue cells within the tumor microenvironment [19]. This study showed preferential binding of exosomes from the cancer plasma to carbon beads. Other sources of exosomes are expected in the plasma of an individual, including cancer patients. If the carbon beads captured the healthy exosomes this could lead to untoward effects, resulting in benefit to the cancer cells. In this regard, this study is highly significant for targeted therapy for solid tumors.

The findings are intriguing since the data suggest intervention with an extracorporeal filtration system. This would allow for the removal of communicating exosomes to mitigate the pathological effects of the tumor cells. We envision both adjuvant and neoadjuvant use of carbon in cancer treatment. The use of carbon would not change the treatment but could enhance standard treatment and perhaps prolong the state of remission. This is particularly important for cancers with poor prognosis such as GBM and ovarian [20, 21]. This study has significant data to rationalize a larger study with cancer cell lines as well as patient samples. A larger study with other cancers – solid and hematological – would benefit from this type of treatment.

An interesting finding is the comparison of breast cancer that was HER2+ and TNBC. It was interesting that HER2+ breast cancer adhered to carbon. However, we did not observe similar results with TNBC (Figure 6). This led us to question whether the HER2 receptor could be a target to capture breast cancer cells on C529 carbon. Although these are single patient samples, the outcome underscores the need for a larger study.

The experimental study noted that efficient binding could be a function of the incubation time and number of exosomes (Figure 2). These findings will form the basis for future studies to determine the conditions required to treat cancer. There will be considerations based on the stage of the cancer, whether the patient has undergone treatment, and cancer recurrence. The beads did not bind negatively charged DNA. Exosomes might be hydrophobic or negatively or positively charged, depending on the expressed molecules. It is possible that the binding might not depend on charge since the carbon is hydrophobic.

An advantage of proposing synthetic carbon beads is their ability to offer a compelling platform for exosome capture due to their higher surface area, customizable pore structure, and physiochemical properties that favor molecular absorption. Activated carbon has been revered in the biomedical and industrial filtration system industries because of its biocompatibility and

ability to bind to a diverse array of biological molecules, including proteins and lipids. The data support application of the porous carbon beads to serve as an effective, passive capture system for circulating exosomes, perhaps through specific surface interaction. This approach may provide a scalable and non-invasive method to reduce the burden of tumor-promoting exosomes.

In summary, the findings showed the potential to utilize carbon particles, perhaps with an extracorporeal filtration system to mitigate the major cancer communication exosomes. This will allow slow growth of cancer for a better outcome with standard treatment. It was interesting that the number of bound particles reduced following surgery in the patient with ovarian cancer. This strongly suggests that the bound exosomes were cancer derived since the tumor burden was decreased with surgery. Similarly, chemotherapy brought the levels of bound exosomes to those of healthy control.

## **Funding**

This study was funded by donations to BioCeptor Medical Research Corp.

## **Acknowledgement**

We thank Dr. Caitlyn Moore for assisting with the SEM studies.

## **Conflict of Interest**

The authors declare no potential conflict of interest.

## **References**

- [1] Bang, C., and T. Thum. 2012. Exosomes: new players in cell–cell communication. *The Intl J Viochem Cell Biol* 44: 2060–2064.
- [2] Sandiford, O. A., R. J. Donnelly, M. H. El-Far, L. M. Burgmeyer, G. Sinha, S. H. Pamarthi, L. S. Sherman, A. I. Ferrer, D. E. DeVore, S. A. Patel, Y. Naaldijk, S. Alonso, P. Barak, M. Bryan, N. M. Ponzio, R. Narayanan, J. P. Etchegaray, R. Kumar, and P. Rameshwar. 2021. Mesenchymal Stem Cell-Secreted Extracellular Vesicles Instruct Stepwise Dedifferentiation of Breast Cancer Cells into Dormancy at the Bone Marrow Perivascular Region. *Cancer Res* 81: 1567–1582.

- [3] Walker, N. D., M. Elias, K. Guiro, R. Bhatia, S. J. Greco, M. Bryan, M. Gergues, O. A. Sandiford, N. M. Ponzio, S. J. Leibovich, and P. Rameshwar. 2019. Exosomes from differentially activated macrophages influence dormancy or resurgence of breast cancer cells within bone marrow stroma. *Cell Death Dis* 10: 59.
- [4] Bliss, S. A., G. Sinha, O. A. Sandiford, L. M. Williams, D. J. Engelberth, K. Guiro, L. L. Isenalumhe, S. J. Greco, S. Ayer, M. Bryan, R. Kumar, N. M. Ponzio, and P. Rameshwar. 2016. Mesenchymal Stem Cell-Derived Exosomes Stimulate Cycling Quiescence and Early Breast Cancer Dormancy in Bone Marrow. *Cancer Res* 76: 5832–5844.
- [5] Greco, S. J., S. Ayer, K. Guiro, G. Sinha, R. J. Donnelly, M. H. El-Far, L. S. Sherman, Y. Kenfack, S. H. Pamarthi, M. Gergues, O. A. Sandiford, M. J. Schonning, J. P. Etchegaray, and P. Rameshwar. 2021. Restoration of aged hematopoietic cells by their young counterparts through instructive microvesicles release. *Aging (Albany NY)* 13: 23981–24016.
- [6] Buschow, S. I., B. W. Van Balkom, M. Aalberts, A. J. Heck, M. Wauben, and W. Stoorvogel. 2010. MHC class II-associated proteins in B-cell exosomes and potential functional implications for exosome biogenesis. *Immunol cell Biol* 88: 851–856.
- [7] Sun, B., P. Dalvi, L. Abadjian, N. Tang, and L. Pulliam. 2017. Blood neuron-derived exosomes as biomarkers of cognitive impairment in HIV. *Aids* 31: F9–F17.
- [8] Paskeh, M. D. A., M. Entezari, S. Mirzaei, A. Zabolian, H. Saleki, M. J. Naghdi, S. Sabet, M. A. Khoshbakht, M. Hashemi, and K. Hushmandi. 2022. Emerging role of exosomes in cancer progression and tumor microenvironment remodeling. *J Hematol Oncol* 15: 83.
- [9] Kalluri, R. 2016. The biology and function of exosomes in cancer. *J Clin Invest* 126: 1208–1215.
- [10] Potian, J. A., H. Aviv, N. M. Ponzio, J. S. Harrison, and P. Rameshwar. 2003. Veto-like activity of mesenchymal stem cells: functional discrimination between cellular responses to alloantigens and recall antigens. *J Immunol* 171: 3426–3434.
- [11] Munoz, J. L., S. A. Bliss, S. J. Greco, S. H. Ramkissoon, K. L. Ligon, and P. Rameshwar. 2013. Delivery of Functional Anti-miR-9 by Mesenchymal Stem Cell-derived Exosomes to Glioblastoma Multiforme Cells Conferred Chemosensitivity. *Mol Ther Nucleic Acids* 2: e126.
- [12] Xu, X., F. Yin, M. Guo, G. Gan, G. Lin, C. Wen, J. Wang, P. Song, J. Wang, Z. Q. Qi, and C. Q. Zhong. 2023. Quantitative proteomic analysis

- of exosomes from umbilical cord mesenchymal stem cells and rat bone marrow stem cells. *Proteomics* 23: e2200204.
- [13] Liu, S.-L., P. Sun, Y. Li, S.-S. Liu, and Y. Lu. 2019. Exosomes as critical mediators of cell-to-cell communication in cancer pathogenesis and their potential clinical application. *Transl Cancer Res* 8: 298.
- [14] Anker, P., H. Mulcahy, X. Qi Chen, and M. Stroun. 1999. Detection of circulating tumour DNA in the blood (plasma/serum) of cancer patients. *Cancer Met Rev* 18: 65–73.
- [15] Thakur, B. K., H. Zhang, A. Becker, I. Matei, Y. Huang, B. Costa-Silva, Y. Zheng, A. Hoshino, H. Brazier, and J. Xiang. 2014. Double-stranded DNA in exosomes: a novel biomarker in cancer detection. *Cell Res* 24: 766–769.
- [16] Gemel, J., J. Kilkus, G. Dawson, and E. C. Beyer. 2019. Connecting Exosomes and Connexins. *Cancers* 11: 476.
- [17] Soares, A. R., T. Martins-Marques, T. Ribeiro-Rodrigues, J. V. Ferreira, S. Catarino, M. J. Pinho, M. Zuzarte, S. Isabel Anjo, B. Manadas, J. P.G. Sluijter, P. Pereira, and H. Girao. 2015. Gap junctional protein Cx43 is involved in the communication between extracellular vesicles and mammalian cells. *Sci Reports* 5: 13243.
- [18] Norris, R. P. 2021. Transfer of mitochondria and endosomes between cells by gap junction internalization. *Traffic* 22: 174–179.
- [19] Record, M., K. Carayon, M. Poirot, and S. Silvente-Poirot. 2014. Exosomes as new vesicular lipid transporters involved in cell–cell communication and various pathophysiological processes. *Biochimica et Biophysica Acta (BBA)-Mol Cell Biol Lipids* 1841: 108–120.
- [20] Zhang, P., Q. Xia, L. Liu, S. Li, and L. Dong. 2020. Current opinion on molecular characterization for GBM classification in guiding clinical diagnosis, prognosis, and therapy. *Frontiers Mol Biosci* 7: 562798.
- [21] Au, K. K., J. A. Josahkian, J.-A. Francis, J. A. Squire, and M. Koti. 2015. Current state of biomarkers in ovarian cancer prognosis. *Future Oncol* 11: 3187–3195.

